

A haemocompatible and scalable nanoporous adsorbent monolith synthesised using a novel lignin binder route to augment the adsorption of poorly removed uraemic toxins in haemodialysis

This content has been downloaded from IOPscience. Please scroll down to see the full text.

Download details:

IP Address: 128.41.35.98

This content was downloaded on 14/03/2017 at 14:12

Manuscript version: Accepted Manuscript

Sandeman et al

To cite this article before publication: Sandeman et al, 2017, Biomed. Mater., at press:

<https://doi.org/10.1088/1748-605X/aa6546>

This Accepted Manuscript is: © 2017 IOP Publishing Ltd

As the Version of Record of this article is going to be / has been published on a gold open access basis under a CC BY 3.0 licence, this Accepted Manuscript is available for reuse under a CC BY 3.0 licence immediately.

Everyone is permitted to use all or part of the original content in this article, provided that they adhere to all the terms of the licence <https://creativecommons.org/licences/by/3.0>

Although reasonable endeavours have been taken to obtain all necessary permissions from third parties to include their copyrighted content within this article, their full citation and copyright line may not be present in this Accepted Manuscript version. Before using any content from this article, please refer to the Version of Record on IOPscience once published for full citation and copyright details, as permissions will likely be required. All third party content is fully copyright protected, unless specifically stated otherwise in the figure caption in the Version of Record.

When available, you can view the Version of Record for this article at:

<http://iopscience.iop.org/article/10.1088/1748-605X/aa6546>

1
2
3 A haemocompatible and scalable nanoporous adsorbent monolith synthesised using a novel
4 lignin binder route to augment the adsorption of poorly removed uraemic toxins
5

6 Susan R. Sandeman^{1*}, Yishan Zheng¹, Ganesh C. Ingavle¹, Carol A. Howell¹, Sergey V.
7 Mikhalovsky¹, Kolitha Basnayake², Owen Boyd³, Andrew Davenport⁴, Nigel Beaton⁵, Nathan
8 Davies⁵
9
10

11
12
13 ¹Biomaterials and Medical Devices Research group, School of Pharmacy and Biomolecular
14 Sciences Huxley Building, University of Brighton, Brighton, BN2 4GJ, UK
15

16
17 ²Sussex Kidney Unit, ³Intensive Care Unit, Brighton & Sussex University Hospitals NHS Trust,
18 Brighton, BN2 5BE, UK
19

20
21 ⁴UCL Centre for Nephrology, ⁵UCL Institute for Liver and Digestive Health, Royal Free Campus,
22 Roland Hill Street, London NW3 2PF, UK
23
24
25
26
27

28 *Susan Sandeman, Ph. D. (Corresponding Author)

29
30 Biomaterials and Medical Devices Research Group, School of Pharmacy and Biomolecular
31 Sciences, Huxley Building, University of Brighton, Brighton BN2 4GJ, UK
32
33

34 Phone: +44 01273 641377
35

36 E-mail: s.sandeman@brighton.ac.uk
37
38
39
40
41
42
43
44
45
46
47
48
49
50
51
52
53
54
55
56
57
58
59
60

Abstract

Nanoporous adsorbents are promising materials to augment the efficacy of haemodialysis for the treatment of end stage renal disease where mortality rates remain unacceptably high despite improvements in membrane technology. Complications are linked in part to inefficient removal of protein bound and high molecular weight uremic toxins including key marker molecules albumin bound indoxyl sulphate (IS) and p-cresyl sulphate (PCS) and large inflammatory cytokines such as IL-6. The following study describes the assessment of a nanoporous activated carbon monolith produced using a novel binder synthesis route for scale up as an in line device to augment haemodialysis through adsorption of these toxins. Small and large monoliths were synthesised using an optimised ratio of lignin binder to porous resin of 1 in 4. Small monoliths showing combined significant IS, p-CS and IL-6 adsorption were used to measure haemocompatibility in an *ex vivo* healthy donor blood perfusion model, assessing coagulation, platelet, granulocyte, t cell and complement activation, haemolysis, adsorption of electrolytes and plasma proteins. The small monoliths were tested in a naive rat model and showed stable blood gas values, blood pressure, blood biochemistry and the absence of coagulopathies. These monoliths were scaled up to a clinically relevant size and were able to maintain adsorption of protein bound uremic toxins IS, PCS and high molecular weight cytokines TNF- α and IL-6 over 60 minutes using a flow rate of 300 mL/min without platelet activation. The nanoporous monoliths were haemocompatible and retained adsorptive efficacy on scale up with negligible pressure drop across the system indicating potential for use as an in-line device to improve haemodialysis efficacy by adsorption of otherwise poorly removed uraemic toxins.

Key words

Nanoporous, activated carbon, uraemic toxins, haemodialysis, end stage renal disease

1. Introduction

Nanoporous adsorbents offer a potential method by which to address the life-reducing complications associated with poor removal of protein bound and high molecular weight uraemic toxins during haemodialysis. Whilst more than two million patients with end stage renal disease (ESRD) are treated by haemodialysis worldwide mortality rates remain high. Almost half of all patients who receive a diagnosis of ESRD die within three years, most commonly as a result of cardiovascular co-morbidity followed by infection (1-4). Haemodialysis is a life sustaining therapy and an efficient method for removing excess fluid and highly water soluble small molecules such as ionic solutes and urea from blood. Urea is known to hydrolyse into cyanate and form carbamylated haemoglobin (5-8) and other carbamylated proteins and lipoproteins. However, there is debate as to whether urea is a “uraemic” toxin or whether its use as a marker of dialysis adequacy actually correlates with adequate removal of uraemic toxins with the most damaging effects on tissue physiology (9, 10). Urea is rapidly cleared during standard haemodialysis whereas other uraemic retention solutes, particularly protein bound and high molecular weight molecules, are minimally cleared resulting in retention in ESRD patients (11). Indoxyl sulphate (IS) and p-cresyl sulphate (PCS) are protein bound uraemic toxins derived from protein metabolism (12). They have been shown, both within in vitro and in animal models, to cause endothelial damage and cardiovascular disease, and are associated with increased mortality in ESRD patients (12-17). To date a suitable method to remove these and the many other poorly removed protein bound and high molecular uraemic toxins (17) remains to be found (11, 18).

Addition of an adsorption device into the standard haemodialysis circuit has great potential to improve removal of such toxins (2, 19-23). Synthetic, activated carbon adsorbents offer

1
2
3 considerable advantages over other polymer based systems. They outperform other
4 adsorbents through the existence of a highly developed internal surface area which is
5 suitable for non-specific adsorption of predominantly hydrophobic, organic molecules. Early
6 studies using various granular AC formulations from a range of natural sources showed
7 some success but were ultimately constrained by variable performance, poor
8 haemocompatibility particularly related to platelet loss, pressure drop and poor adsorption
9 of larger biological molecules when coated (24-31). Advances in production technology
10 using synthetic pre-cursors have improved activated carbon performance through carefully
11 controlled formulation, carbonisation and activation procedures allowing the production of
12 mechanically strong microbeads with an internal surface area of over $1500 \text{ m}^2\text{g}^{-1}$ (32-34).
13 Additionally it is possible to significantly increase capacity for the removal of protein bound
14 and high molecular weight uraemic toxins through the development of nanopores with
15 diameter in the range of 10-100 nm (35-38). This structure can be maintained and potential
16 for pressure drop reduced by the production of activated carbon monoliths, formed as
17 extruded cylinders with numerous micro-diameter channels along which blood flows. We
18 have previously shown that nanoporous activated carbon monoliths can adsorb protein
19 bound uraemic and high molecular weight toxins which are poorly removed by
20 haemodialysis alone (39). However, a monolith synthesis route which enabled the
21 production of monoliths with attrition resistance and adsorptive capacity on scale up to a
22 clinically relevant size was not possible using the previous synthesis route. The aim of the
23 current study was to assess monoliths produced by a novel lignin binder route for
24 haemocompatibility using ex vivo healthy donor and a naive rat haemoperfusion model.
25 Maintenance of nanoporosity and adsorptive capacity on scale up was then assessed with
26 the ultimate goal of providing a potential augmentation strategy for haemodialysis.
27
28
29
30
31
32
33
34
35
36
37
38
39
40
41
42
43
44
45
46
47
48
49
50
51
52
53
54
55
56
57
58
59
60

2. Materials and Methods

2.1 Monolith synthesis

Monoliths were synthesised using a novolac phenol-formaldehyde resin pre-cursor dissolved in a pore-forming solvent, ethylene glycol, together with a cross-linking agent, hexamethylenetetramine, and lignin binder. The ratio of lignin binder to nanoporous resin was optimised to a wt% ratio of 25:75. The pre-polymer solution was cured and the resulting resin cake was crushed, washed and dried to remove excess pore former then milled and formed into a dough for extrusion. The resulting monoliths were carbonised at 700 °C and activated in carbon dioxide at temperatures of up to 880°C. Nanoporosity was controlled primarily by initial resin pore-former composition and the unique phase separation that occurs during the curing stage. Small monoliths were prepared with a diameter of 7 mm, length of 95 mm and contained 30 square micro-channels. Large monoliths were prepared with a diameter of 30 mm and length of 225 mm and contained 600 square micro-channels with a diameter of 300 µm. The monoliths were encased in heat shrink polyolefin tubes supplied by RS Components Ltd (Northamptonshire, UK). The process sealed Leuer lock fittings to the ends of the monoliths prior to the perfusion studies (fig 1a and 1b).

2.2 Physical characterisation of small and large monoliths

The surface and internal porous morphology of the resultant monolithic materials were characterised by scanning electron microscopy (SEM) using a Sigma field emission gun

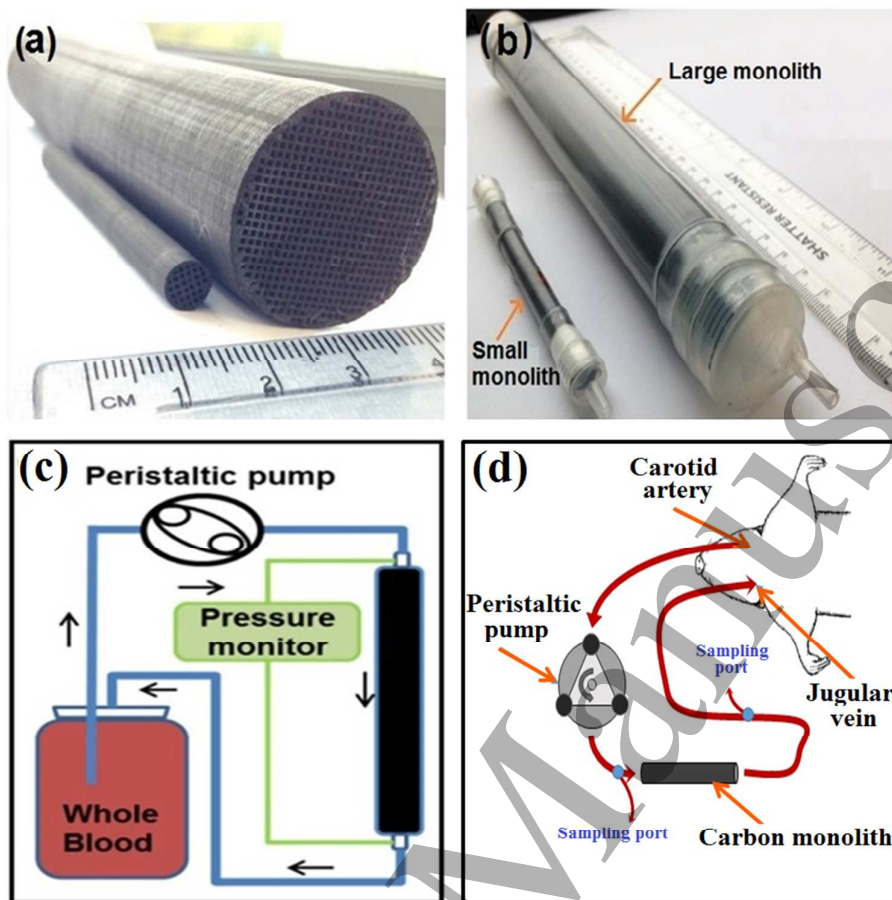


Figure 1 (a) Small and large monoliths were produced using a novel lignin binder route with dimensions of 0.7 cm x 9.5 cm and 2.8 x 22.5 cm (diameter by length) and microchannel numbers of 30 channels and 600 channels respectively (b) The monoliths were encased in heat shrink polyolefin tubes (c) In vitro plasma and whole blood experiments were conducted, perfusing fluid through the monolith microchannels at a flow rate of 5ml/min for the small monolith studies and 300 ml/min for the large monolith studies (d) A naive rat haemoperfusion model was used to carry out an in vivo safety assessment of the small monoliths

(FEG)-SEM microscope (Carl Zeiss NTS, Cambridge, UK). The definition of pore size in nanoporous materials according to the International Union of Pure and Applied Chemistry (IUPAC) is that micropores are smaller than 2 nm in diameter, mesopores 2-50 nm and macropores larger than 50 nm. The carbons used in this study were predominantly micro-macroporous. Prior to measurement, the hierarchically porous monolithic materials were

1
2
3 dried under vacuum at 150°C overnight. The pore size distribution data was determined
4
5 using a PoreMaster mercury intrusion porosimeter (Quantachrome Instruments Ltd, Hook,
6
7 UK). Surface area was determined using an Autosorb-1 gas sorption analyser,
8
9 (Quantachrome Instruments, USA) using Quantachrome data analysis software
10
11 (Quantachrome ASiQwin) and the Brunauer, Emmett and Teller (BET) method.
12
13

14 **2.3 Adsorption of marker uraemic toxins by the small monoliths**

15
16 The small monoliths were primed with saline solution for 30 minutes at a flow rate of 5
17
18 ml/min. A 20 ml volume of fresh frozen human plasma (Cambridge Bioscience) was spiked
19
20 with IS (125 µM), PCS (250 µM) and IL6. The spiked plasma solution underwent continuous
21
22 circulation through the monoliths and samples were collected over time. IS and PCS
23
24 concentrations were measured by HPLC using a method described in (39) and IL6
25
26 concentration was measured by ELISA according to manufacturer's instructions using a
27
28 plasma dilution of 1:5 (BD Biosciences).
29
30
31
32

33 **2.4 Haemocompatibility testing of small monoliths**

34
35 Haemocompatibility studies were carried out according to ISO standard 10993-4:2002 (E)
36
37 using freshly drawn healthy donor blood from an anonymised healthy donor database held
38
39 by the NIHR Brighton & Sussex Clinical Research Facility using informed consent protocols
40
41 (UK National Research Ethics System (NRES) Committee South East Coast – Brighton and
42
43 Sussex REC reference 13/LO/1058). The small monoliths (7 mm x 95 mm with 30 micro-
44
45 channels) were pre-conditioned with saline (0.9% NaCl) for 30 minutes prior to continuous
46
47 circulation of 20 ml of healthy donor blood through the monoliths for 60 minutes at a flow
48
49 rate of 5 mL/minute (fig 1c). Plasma was prepared by centrifugation of blood samples at
50
51 3500 rpm for 15 minutes.
52
53
54
55

56 **2.5 Complement activation**

57
58
59
60

1
2
3 The presence of C3a, C4a and C5a was measured in plasma prepared from EDTA
4 anticoagulated blood by enzyme linked immunosorbent assay (ELISA) (BD Biosciences).
5
6
7 ELISAs were carried out according to manufacturer's instructions issuing a 1 in 2000 dilution
8
9
10 for C3a and C4a and a 1 in 40 dilution for C5a.
11

12 **2.6 Platelet activation**

13
14 The presence of PAC-1 and CD62 platelet activation markers (BD Biosciences UK) was
15 measured in sodium citrate anticoagulated donor blood samples pre- and post- perfusion
16
17 through monolith and tubing only controls using flow cytometry. The first 2 mL blood was
18
19 drawn and discarded. 2 mL of blood incubated with ADP (2 μ M) (Sigma Aldrich, UK) for 5
20
21 minutes was used as a positive control. Fresh whole blood samples (5 μ L) were incubated in
22
23 the dark with PE/CD61 (10 μ L), APC /D62P (10 μ L) and FITC/PAC-1 (10 μ L) antibody cocktail
24
25 for 20 minutes, fixed using chilled 1% paraformaldehyde in PBS (1 mL) for 30 minutes at 4 °C
26
27 and analysed using an Accuri C6 flow cytometer and BD CSampler software (version
28
29 1.0.264.21). The flow cytometer was set to slow flow rate, with a forward scatter (FSC)
30
31 threshold of 10'000 to collect 10'000 events on the platelet gate.
32
33
34
35
36
37

38 **2.7 Granulocyte activation**

39
40 Granulocyte activation was measured by testing lithium heparin anticoagulated donor blood
41
42 samples for the presence of CD14/CD11b markers (Biolegend, UK) using flow cytometry.
43
44 Positive control samples were prepared by incubating blood samples with interleukin 6 (IL-
45
46 6) (50 ng/mL) and interleukin 8 (IL-8) (50 ng/mL) for 60 minutes. Blood samples (100 μ L)
47
48 were incubated with PE/CD14 (20 μ L) and APC/CD11b (20 μ L) antibody cocktails for 20
49
50 minutes. Stained blood samples were incubated with lyse/fix buffer (1.5 mL) in the dark for
51
52 30 minutes prior to centrifugation at 600g for 6 min, removal of supernatant and washing of
53
54 cells in 2 mL stain buffer. Cells were pelleted and resuspended in 300 μ L stain buffer for
55
56
57
58
59
60

1
2
3 analysis using flow cytometry. The flow cytometer was set to medium flow rate, with a
4 forward scatter (FSC) threshold of 80'000 to collect 10'000 events.
5
6

7 8 **2.8 T cell activation**

9
10 T cell activation was assessed in EDTA anticoagulated blood samples by measuring the
11 activation of STAT3 and STAT 5 intracellular phosphorylation pathways using flow
12 cytometry. Whole blood samples (200 μ L) were lysed, permeabilised and stained by
13 incubating with PerCP/CD3, Alexa488/CD8, PE/CD4 antibody cocktail (20 μ L) and
14 Alexa647/STAT3 or STAT5 (20 μ L) for 1 hour. Positive control samples were prepared using
15 an IL-6 (50 ng/mL) and IL-8 (50 ng/mL) spike for STAT3 activation and interleukin 2 (IL-2) (50
16 ng/ml) spike for STAT5 activation followed by incubation for 60 minutes. Cells were washed
17 and resuspended in 200 μ L stain buffer for analysis using flow cytometry with setting as for
18 the granulocyte activation assay.
19
20
21
22
23
24
25
26
27
28
29

30 31 **2.9 Adsorption of uraemic toxins by the large monoliths**

32
33 Large monoliths (n=3) were pre-conditioned with intravenous infusion saline solution (0.9%
34 NaCl, 0.15% KCl & 0.2% MgCl) (Baxter) for 30 minutes. A 400 mL volume of blood, anti-
35 coagulated with sodium heparin and commercially supplied by Cambridge Biosciences, was
36 spiked with 1000 pg/mL IL-6 and tumor necrosis factor alpha (TNF- α), 125 μ M IS and 250
37 μ M PCS and continuously perfused through the monolith or tubing controls for 60 minutes
38 at a flow rate of 300 ml/min (LaboVAR 225 pump, Möller Medical GmbH Fulda Germany).
39 Samples were collected after 0, 5, 30, 60 min. IS and PCS concentrations were measured by
40 HPLC using a method described in (39) and IL6/TNF- α concentration was measured by
41 ELISA according to manufacturer's instructions using a dilution of 1:5 (BD Biosciences).
42
43
44
45
46
47
48
49
50
51
52
53
54
55
56
57
58
59
60
Platelet activation was measured in the plasma derived from the timed blood samples as
described in section 2.5.

2.11 In vivo safety assessment of small monoliths

All studies were conducted under the governance of the UK Animals in Scientific Procedures Act (1986, amended 2012), with full local ethical approval. Animals were allowed free access to food and water prior to the study and housed under a 12 hour light/dark cycle at 20°C (+/-2°C). Adult male Sprague-Dawley rats (250-300 g, Charles River UK) were anaesthetised under isoflurane (induction at 5% in oxygen, maintenance at 1.5% in air for the duration of the study) and had catheters placed in the left carotid artery and right jugular vein. Mean arterial pressure was recorded at hourly intervals (Biopac US) and core body temperature recorded throughout the study. To maintain body temperature, the animals were maintained on regulated heat mats and covered with insulated materials as required.

Blood samples were collected into lithium heparin coated tubes for blood gas analysis (Siemens Medical Diagnostics, UK) and plasma biochemistry prior to, and at hourly intervals throughout the study. After an initial 30 minute stabilisation period, the arterial catheter was connected to a carbon monolith (approximately 10cm by 1cm (length x diameter)) via a peristaltic pump (figure 1d). The blood was then returned to the animal via the catheter placed into the jugular vein. Flow rates throughout the 2-hour treatment period were set at 2 ml/min with the total circuit volume not exceeding 10% of the circulating blood volume of the animal (ca. 3 ml maximum). The circuit was pre filled with heparinised saline solution (1000 U/L), with a saline bolus (ca. 2 ml) administered to the animal at the start of treatment to prevent hypotension. At the termination of the study, blood and tissue samples were collected under terminal anaesthesia. Blood samples for biochemistry were stored on ice before centrifugation (3500 rpm, 10 min, 4 °C) and storage at -80°C. Plasma

1
2
3 biochemistry (glucose, urea, albumin, total protein, ALT, AST, creatinine) was assessed using
4
5 an automated COBAS system (Roche, UK) following manufacturer's instructions.
6
7

8 9 **2.10 Statistical analysis**

10 Statistical analysis was carried out using GraphPad Prism 6.05 software and two-way ANOVA
11
12 with Tukey's multiple comparison tests.
13
14

15 16 **3. Results**

17 18 **3.1 Physical characterisation of the large and small monoliths**

19
20 The synthesis and activation process resulted in a well-defined distribution of transport
21
22 microchannels running in parallel along the length of the monoliths (fig 2a-c). The internal
23
24 structure of the carbon monolith walls was visible in the SEMs as larger macroporous and
25
26 smaller nanoporous domains. The mercury porosimetry pore size distribution plot indicated
27
28 nanoporous domains in the 20-100 nm range in both the small and large monoliths with
29
30 mean peak porosity of 55.6 nm and 62.1 nm respectively (fig 2d). The BET surface area was
31
32 calculated by gas nitrogen porosimetry to be 1117 m² g⁻¹ in the small monoliths and 1056
33
34 m² g⁻¹ in the large monoliths.
35
36
37
38
39
40
41
42
43
44
45
46
47
48
49
50
51
52
53
54
55
56
57
58
59
60

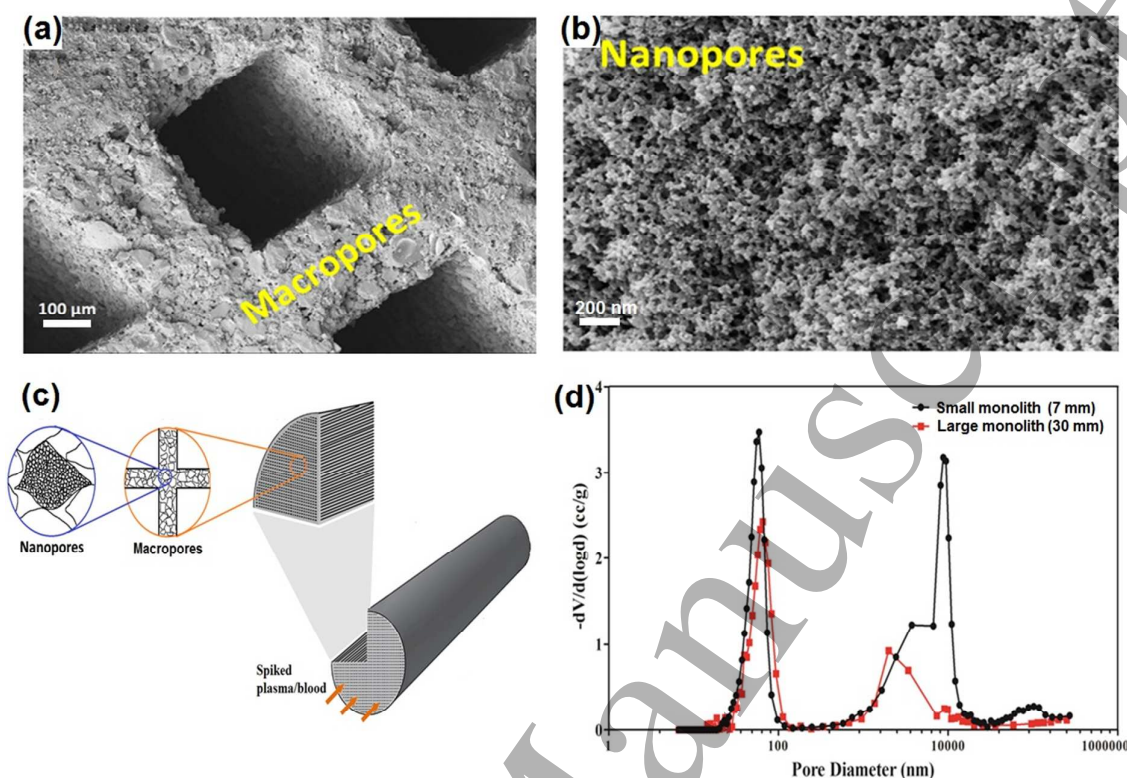


Figure 2 (a) Scanning electron micrograph showing microchannel geometry and (b) nanoporous domains within the walls of the small and large monoliths (c) Mercury pore size distribution plots indicated consistent meso-macroporosity in the small and large monoliths with a mean pore size of 56 nm and 62 nm respectively and S_{BET} surface area calculated by gas nitrogen porosimetry of 1117 and 1056 m^2/g respectively

3.2 Adsorption of marker uraemic toxins by the small monoliths

The small monoliths synthesised using a 25% lignin binder were able to adsorb uraemic toxins IS and PCS, reducing them to negligible levels and reduced IL-6 concentration by 80% (fig 3).

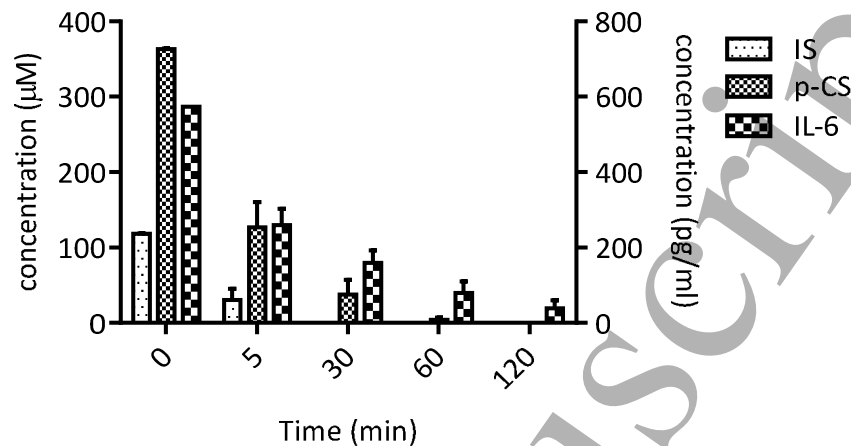


Figure 3 Adsorption of IS (125 μ M), p-CS (250 μ M) and IL-6 (1000 pg/ml) from spiked fresh frozen human plasma over time by the small monoliths synthesised using a 25:75 %wt ratio of lignin to nanoporous resin (n=3, mean+/-SEM)

3.3 Haemocompatibility testing of the small monoliths

3.3.1. Complement activation

Blood perfused through the small monoliths over time did not cause significant complement activation when compared to the negative, tubing only control ($p > 0.05$) (Fig 4a-c). Some complement activation was observed at baseline and a slight increase occurred in both the monolith and tubing only controls over the 60 minute perfusion cycle. However, this was significantly less than that of the zymosan A activated positive controls in which complement fragment concentrations increased from 1.5 ng/mL to 4.1 ng/mL for C3a ($p < 0.0001$) (fig 4a), 1.6 ng/mL to 3.3 ng/mL for C4a ($p < 0.05$) (fig 4b) and 3.9 pg/mL to 43.5 pg/mL for C5a ($p < 0.0001$) (Fig. 4c). C5a concentration detected in the plasma was in the picogram range and significantly lower than that for C3a and C4a which was in the ng range.

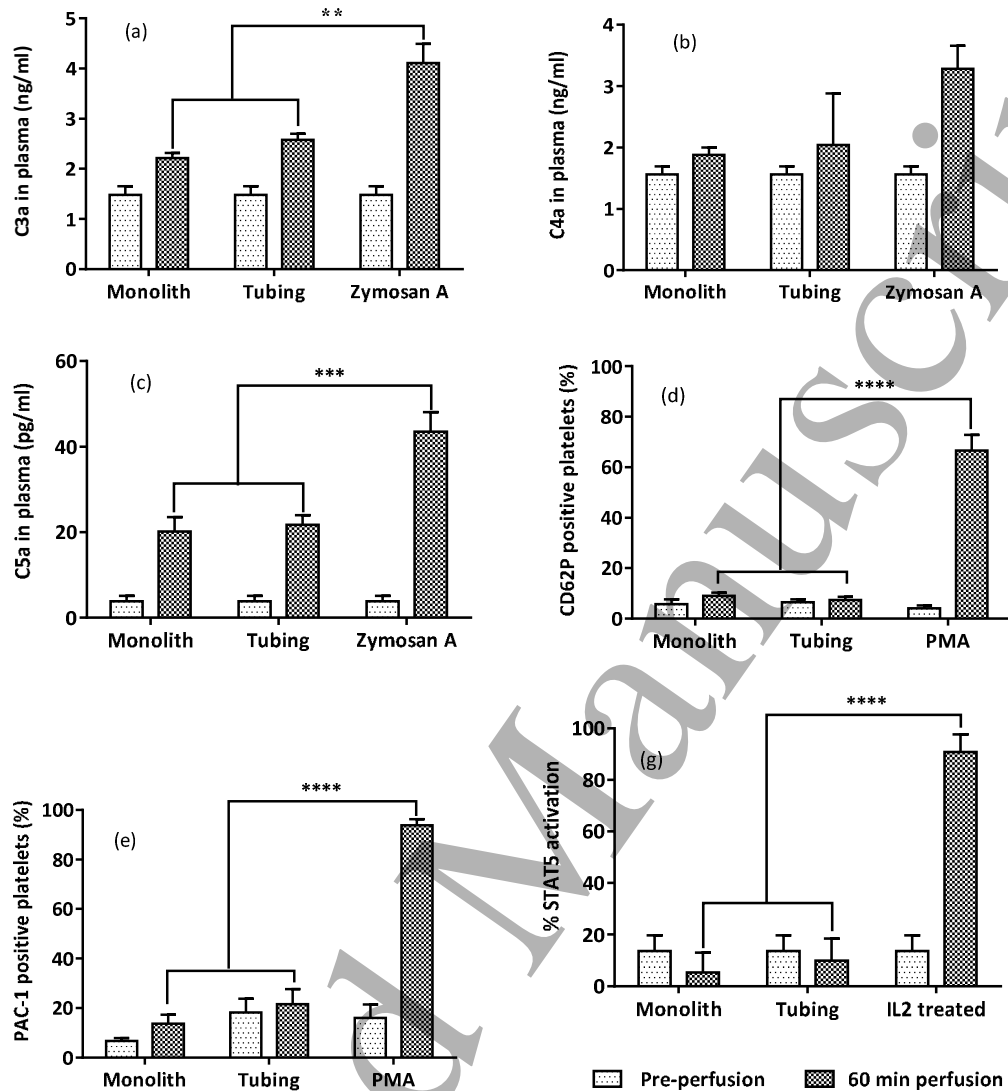


Figure 4 Perfusion of freshly drawn healthy donor blood through the small monoliths over 60 minutes stimulated no significant complement activation measured using (a) C3a (b) C4a and (c) C5a activation markers, no significant platelet activation measured using (d) PAC-1 and (e) CD62P activation markers and no significant T cell activation, measured using phosphorylated (f) STAT3 and (g) STAT5 protein expression when compared to tubing only controls in comparison to the zymosan A, PMA and cytokine stimulated positive controls (mean \pm SEM, n=3), ** $p < 0.01$, **** $p < 0.0001$

3.3.2 Platelet activation

A platelet sub-population was isolated from the total blood cell population using a R-Phycoerythrin (PE) fluorophore conjugated CD61 antibody against the platelet surface

1
2
3 antigen glycoprotein IIIa. Within this platelet sub-population activated platelets were
4
5 detected using a fluorescein isothiocyanate (FITC) fluorophore conjugated PAC-1 antibody
6
7 and an allophycocyanin (APC) conjugated CD62p antibody (fig 4d-e). No significant platelet
8
9 activation occurred following 60 minutes of perfusion through the small monoliths and the
10
11 tubing only controls. No significant difference in the percentage of PAC-1 and CD62P
12
13 positive platelets was observed when comparing the monolith and tubing only control
14
15 following 60 mins continuous filtration through the *ex vivo* circuit. In contrast, the PMA
16
17 (200 nM) spike induced significant platelet activation (SEM \pm , n=3, p<0,0001).
18
19
20
21

22 **3.3.3 Granulocyte activation**

23
24 No significant difference in granulocyte activation was observed between the monolith and
25
26 tubing only controls following 60 minutes perfusion, although granulocyte activation did
27
28 occur in both circuits (data not shown). Granulocyte activation, measured by elevated
29
30 CD11b expression, occurred over 30 and 60 minutes blood perfusion through both
31
32 monoliths and control but was less than that measured in the cytokine stimulated positive
33
34 control (SEM \pm , n=3). 8% granulocyte activation was measured at baseline, 20 \pm 4% after 30
35
36 minutes perfusion and 70 \pm 13% after 60 minutes perfusion in both the small monolith and
37
38 tubing only samples.
39
40
41
42

43 **3.3.4 T cell activation**

44
45 The PE conjugated CD3 antibody was used to identify the T cell subpopulation. Alexa 647
46
47 conjugated STAT3 and STAT5 antibodies were used to identify the post-perfusion, activated
48
49 T cells, IL6/IL8 (50 ng/mL) activated STAT 3 positive control and IL2 activated STAT 5 positive
50
51 control (fig 4f,g). No up regulation of intracellular STAT phosphorylation pathways was
52
53 detected following blood perfusion through the small monoliths over 60 minutes. Negligible
54
55 levels of STAT3 phosphorylation and STAT5 phosphorylation and levels of 10-20% were
56
57
58
59
60

1
2
3 detected in the pre- and post-perfusion monolith samples, tubing only control samples and
4
5 time 0 cytokine spiked positive controls. A significant increase in the cytokine stimulated
6
7 positive control samples occurred over 60 minutes. $91 \pm 3\%$ STAT5 T-cell activation and $64 \pm$
8
9 2% STAT3 T-cell activation was detected. No significant T cell activation, measured by
10
11 phosphorylated STAT3 and STAT5 protein expression, was observed following blood
12
13 perfusion through the monoliths over 60 minutes compared to the cytokine (50 ng/mL)
14
15 stimulated controls (SEM \pm , n = 3, $p < 0.0001$).
16
17
18

19 **3.3.5 Blood biochemistry and coagulometry**

20
21 Haemoglobin and haematocrit values, blood cell count, ionic solutes, urea, creatinine, total
22
23 protein, albumin, fibrinogen and coagulometry measures remained in normal range and
24
25 were not removed significantly by blood perfusion through the small monoliths (Table 1).
26
27 Limited reduction in platelet count, total protein and albumin concentration occurred
28
29 following blood perfusion through the monoliths. Platelet count dropped from 261 ± 54 to
30
31 $230 \pm 75 \times 10^9$ cells/mL post- monolith perfusion. The total protein concentration dropped
32
33 from 75.7 ± 2.5 g/L to 64 ± 2 g/L and albumin concentration dropped from 46 ± 1 to 39.7 ± 0.6
34
35 g/L, all remaining in normal concentration range. A significant reduction in creatinine
36
37 concentration occurred, reducing from 66.7 ± 13.6 to 17.7 ± 6 $\mu\text{mol/L}$. No change in
38
39 activated partial thromboplastin times (aPPT) or International normalised ratio (INR) were
40
41 observed. Fibrinogen concentration reduced from 2.8 g/L in the pre-perfusion blood
42
43 samples to 2.1 g/L in the monolith post perfusion samples but remained within the normal
44
45 reference range.
46
47
48
49
50
51
52
53
54
55
56
57
58
59
60

Table 1. Healthy donor blood perfused through the small monoliths at 5 ml/min for 90 mins did not produce significant changes in blood cell count (WBC, RBC, PLT), haematocrit (HCT) and haemoglobin (HB) measures of haemolysis, urea, creatinine, total protein and APPT and INR measures of coagulation compared to tubing only controls (mean \pm -SD, n=3).

	Pre-perfusion	Monolith	Tubing	Normal range
HB (g/L)	140.8 \pm 16.8	137.2 \pm 30.4	132.8 \pm 26.6	115 - 165
WBC $\times 10^9$ cell/mL	7.4 \pm 1.5	7.4 \pm 2.1	7.9 \pm 2.2	4.0 - 11.0
PLT $\times 10^9$ cell/mL	261 \pm 54	230 \pm 75	288 \pm 111	150 - 450
RBC $\times 10^{12}$ cell/mL	4.76 \pm 0.59	4.57 \pm 1.09	4.40 \pm 0.92	3080 - 5.80
HCT (L/L)	0.416 \pm 0.049	0.381 \pm 0.095	0.365 \pm 0.073	0.350 - 0.470
Sodium (mmol/L)	139 \pm 2	139.7 \pm 0.6	137.0 \pm 1.7	135-146
Potassium (mmol/L)	4.2 \pm 0.2	4.1 \pm 0.1	4.5 \pm 0.2	3.2-5.1
Urea (mmol/L)	4.8 \pm 1.8	3.8 \pm 1.4	4.8 \pm 1.7	1.7-8.3
Creatinine (μmol/L)	66.7 \pm 13.6	17.7 \pm 5.0	69.0 \pm 14.7	62-106
Total protein (g/L)	75.7 \pm 2.5	64 \pm 2	74.7 \pm 1.5	66-87
Albumin (g/L)	46 \pm 1	39.7 \pm 0.6	45.3 \pm 0.6	34-48
Fibrinogen (g/L)	2.8 \pm 0.5	2.1 \pm 0.4	2.8 \pm 0.6	2.0 - 4.0
APTT (S)	1.0 \pm 0.1	1.0 \pm 0.1	0.9 \pm 0.1	0.8 - 1.2
INR	0.1	1.1 \pm 0.1	1.0 \pm 0.0	0.8 - 1.2

3.4 Adsorption of uraemic toxins by the large monoliths

IS and PCS concentrations were reduced from 125 and 250 μ M to negligible levels following perfusion through the large, 30 mm diameter monoliths for 90 minutes compared to the tubing only positive controls where IS and PCS concentration remained unchanged (figure

1
2
3 5a-d). The monoliths adsorbed IL-6 and TNF- α , significantly reducing IL-6 concentration
4
5 from 711 to 162 pg/mL and TNF- α from 1070 to 441 pg/mL over a 90 minute perfusion
6
7 cycle. A platelet activation study showed no significant activation of platelets over 90
8
9 minutes of perfusion through the monoliths and controls (fig 6). A further study extending
10
11 the perfusion cycle to 240 minutes showed continued reduction in IS, PCS and IL-6 (fig 7).
12
13

14 **3.5 In vivo safety assessment of small monoliths**

15
16
17 The in vivo monolith perfusion safety study indicated no major concerns with regard to
18
19 biocompatibility. None of the studies conducted showed any evidence of coagulopathies,
20
21 either in terms of excess bleeding or clotting abnormalities. The circuit was pre-filled with
22
23 heparinised saline, though there was no evidence that the monolith removed heparin from
24
25 the circuit. Blood gas values remained stable throughout the duration of the study (Table
26
27 XX), with only the bicarbonate level showing a moderate decline over the two-hour
28
29 treatment period. This may be due to the amount of saline administered to the animal to
30
31 replace blood volume. Plasma biochemistry values showed decreases in albumin and total
32
33
34
35
36
37
38
39
40
41
42
43
44
45
46
47
48
49
50
51
52
53
54
55
56
57
58
59
60

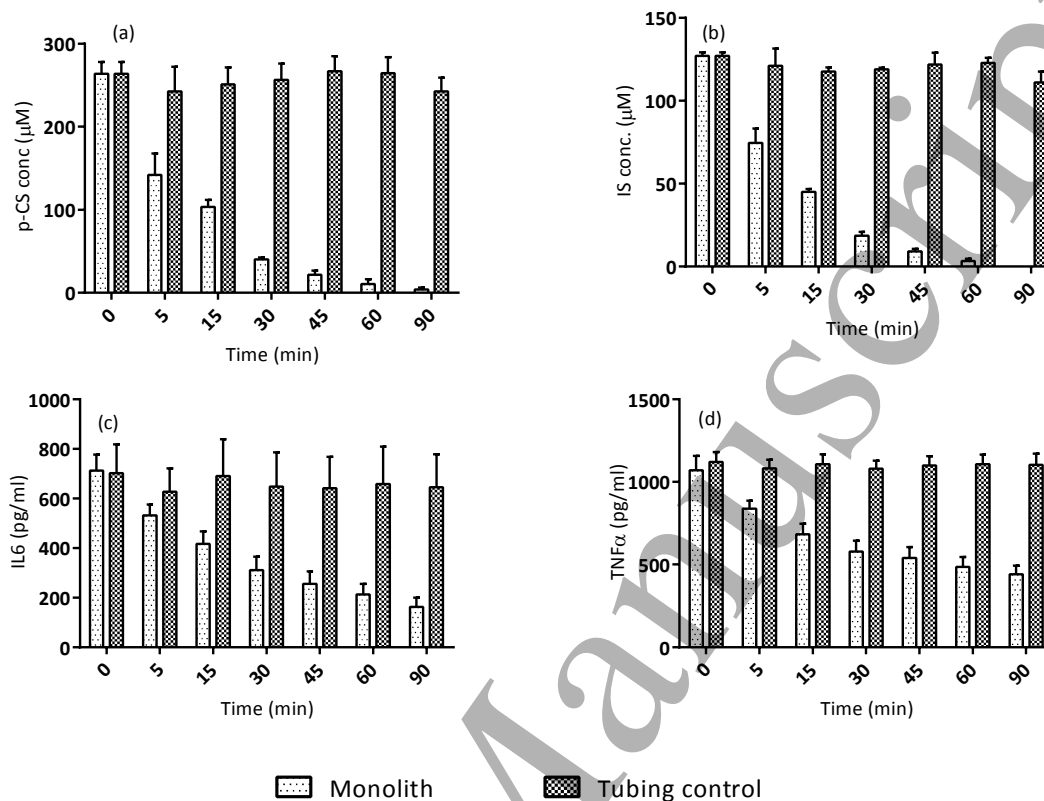


Figure 5 Healthy donor blood spiked with IS ($125 \mu\text{M}$), p-CS ($250 \mu\text{M}$), IL-6 (1000 pg/ml) and TNF(1000 pg/ml) and perfused through the large monoliths at a flow rate of 300 ml/min . (a) IS (b) p-CS (c) IL-6 and (d) TNF- α concentration was significantly reduced following 90 minutes continuous filtration compared to the tubing only control (SEM \pm , n=3), * $p < 0.05$.

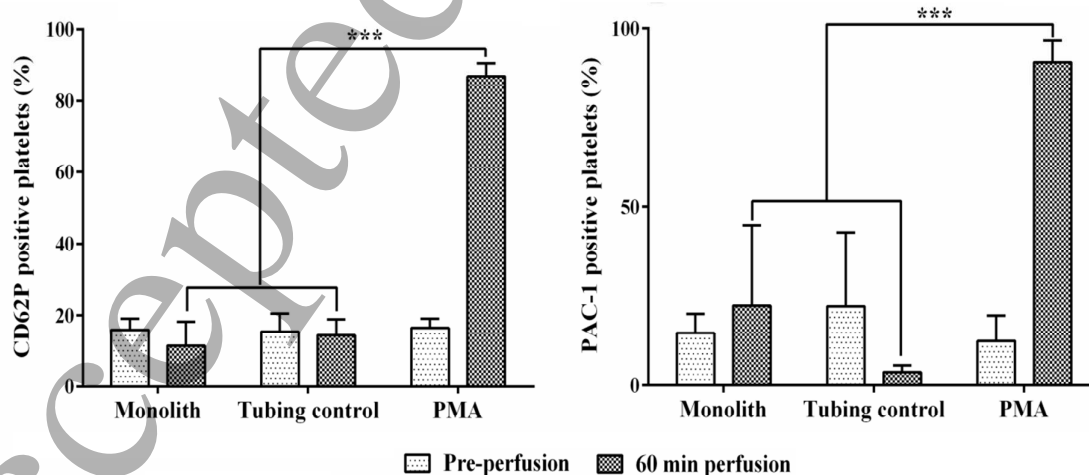


Figure 6 Perfusion of healthy donor blood for 90 minutes through the large monoliths at haemodialysis flow rates did not stimulate platelet activation using (a) PAC-1 and (b) CD62P activation markers compared to tubing only controls. No significant difference in the

percentage of PAC-1 and CD62P positive platelets was observed when comparing the monolith and tubing only control. In contrast, the PMA (200 nM) spike induced significant platelet activation (SEM \pm , n=3), *** p<0.001.

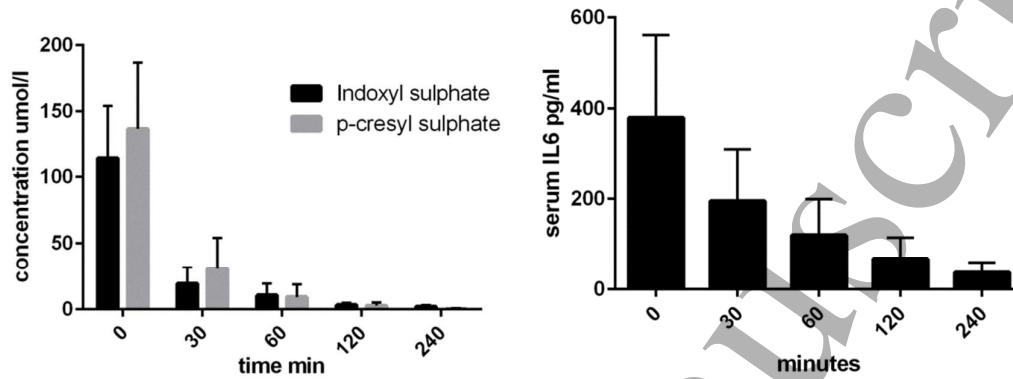


Figure 7 (a) Indoxyl sulphate, p-cresyl sulphate (125 μ M IS, 250 μ M p-CS spike) and (b) IL-6 (1 ng/ml spike) remaining following 240 minutes spiked blood perfusion through the large monoliths (mean \pm SEM, n=8)

protein levels, which may have been due to adsorbance by the column, but are also as a result of the haemodilution caused by connection to the saline filled circuit and additional crystalloid boluses. Creatinine values rose at the end of the study, which may indicate a small degree of haemolysis within the circuit resulting from the continued action of the peristaltic pump. Although this difference in creatinine is significant, the values are not excessively high (Table 2). Mean arterial blood pressure remained stable throughout the duration of the study, indicating that the animals tolerated the procedure well.

Table 2 Naïve rat haemoperfusion data showing the results from blood gas analyses, plasma biochemistry and direct measurement of the mean arterial pressure. Data were analysed using one way ANOVA. * p<0.05, ** p<0.01, ***p<0.001 vs pre-circuit (time 0) values. Data are shown as mean \pm SD, n=9 in each case. Abbreviations, alanine aminotransferase (ALT), aspartate aminotransferase (AST)

	Pre-Circuit	60 mins	120 mins
Blood Gas			
pH	7.4 \pm 0.03	7.4 \pm 0.04	7.4 \pm 0.07

Hematocrit	43.3 ± 0.6	38 ± 2	37.7 ± 3.5
HB (g/dl)	14.7 ± 0.2	13 ± 0.7	12.8 ± 1.1
O ₂ Saturation (%)	96 ± 1.3	96.4 ± 1.3	96.7 ± 0.9
Sodium (mM)	135.4 ± 1.7	135.4 ± 1.6	134.2 ± 1.9
Potassium (mM)	4.3 ± 0.2	4.5 ± 0.3	4.6 ± 0.7
Calcium (mM)	1.3 ± 0.04	1.3 ± 0.05	1.3 ± 0.03
Chlorine (mM)	101.5 ± 1.7	104.7 ± 2.1	104.1 ± 1.8
Glucose (mM)	14.7 ± 3.2	14.2 ± 4	16.8 ± 7.2
Bicarbonate (mM)	26.7 ± 1.1	24.9 ± 2.6	22.8 ± 3.5*

Plasma Biochemistry

Albumin (g/L)	34.4 ± 2.8	26.9 ± 5.4**	25.8 ± 4.1***
Total Protein (g/L)	49.1 ± 1.8	39.5 ± 7.4**	37.3 ± 4.9***
ALT (U/L)	48.9 ± 11.4	36.8 ± 10.4	42.6 ± 12.7
AST (U/L)	67.9 ± 7.4	57.6 ± 15.9	103 ± 81
Creatinine (μM)	20.6 ± 4.5	31.1 ± 8.4	35.6 ± 11.9**

Physiological

Mean Arterial Pressure (mmHg)	98.7 ± 10.6	80.9 ± 17	82.2 ± 28.1
-------------------------------	-------------	-----------	-------------

4. Discussion

The study provides evidence to support the haemocompatibility and efficacy of a scaleable nanoporous activated carbon monolith device for potential use to augment current haemodialysis therapy. A range of haemocompatibility tests using healthy donor blood samples and a small animal blood perfusion modelling study demonstrated that the

1
2
3 monoliths are safe for use in direct blood contact. A novel lignin binder synthesis route was
4
5 used to successfully scale up the device to a clinically feasible size without reducing
6
7 adsorptive efficacy for marker protein bound and high molecular weight uraemic toxins.
8
9
10 Whilst no previous studies on nanoporous activated carbon monoliths with the porous
11
12 range demonstrated in this study have been described, in vitro study data exists for carbons
13
14 in bead form include carbide derived carbons, phenolic resin derived activated carbons and
15
16 carbon incorporated into a mixed matrix hollow fibre membrane form(40-42). The beads
17
18 showed some efficacy in spiked plasma studies but offer no solution to the challenges of
19
20 direct blood contact and pressure drop. Mixed membrane carbon incorporation offers an
21
22 interesting alternative but may limit contact area for sufficient adsorption of high molecular
23
24 weight molecules. In mixed membrane form significant IS and PCS removal was reported but
25
26 no data was reported for high molecular weight species potentially because the membrane
27
28 cut off limits direct contact. Previous studies comparing synthetic resin derived carbon bead
29
30 activation burn off and adsorptive efficacy reported reduction of high molecular weight
31
32 cytokine TNF matching that shown previously for CDCs but data is limited to batch
33
34 adsorption studies from plasma. Within the current study a phenolic resin derived activated
35
36 carbon monolith rather than bead based device was shown to reduce IS and PCS levels in
37
38 spiked whole blood to negligible levels and IL6 and TNF levels by 80% and 60% respectively
39
40 indicating a scaleable efficacy compared to bead based alternatives. The monolith design
41
42 solves issues of haemocompatibility and pressure drop across the adsorbent device without
43
44 resorting to coating with potential subsequent reduction in the molecular weight cut-off and
45
46 adsorptive profile.
47
48
49
50
51
52
53

54 There are many advantages in adapting the activated carbon form to a monolithic structure
55
56 for direct blood perfusion but also many challenges in maintaining porous profile and
57
58
59
60

1
2
3 adsorptive efficacy. Previous tests using a small monolith prototype and haemodialysis
4 patient blood samples indicated that adsorption of protein bound and middle molecules
5 was dependent on creating nanopores in the 2-100 nm range since adsorption of these
6 solutes in carbon monoliths with narrow nanopores of <2 nm was limited (39). The
7 challenge in scaling up the monolith was to maintain nanoporosity but also to design the
8 monolith channel parameters to balance maximum adsorption with appropriate internal
9 fluid dynamics (43). This was achieved in the current device iteration by using a constant 0.3
10 mm microchannel channel size. A short diffusion distance was provided for access to the
11 internal porous surface area in the walls of the monolith and a micro-channel structure
12 capable of minimising shear stress, maintaining laminar flow and thus reducing red blood
13 cell fragility, haemolysis, platelet activation and thrombus formation. Previous studies with
14 activated carbon granules containing narrow nanopores of < 2 nm have highlighted the
15 tendency for excessive pressure drop, platelet consumption, albumin loss and potential for
16 carbon fines release (30). The introduction of a monolithic design was therefore integral to
17 minimise the tendency for flow irregularities, pressure drop and impact on blood cell
18 fragility, platelet loss and protein adhesion.
19

20 Binding of plasma proteins occurs as soon as blood contacts a foreign surface. Dominant
21 plasma proteins albumin, fibrinogen and IgG coat a surface immediately but with a dynamic
22 exchange with other plasma proteins over time (44). Protein surface coating in the
23 extracorporeal circuit becomes problematic if proteins are denatured and expose activation
24 sites for inflammatory pathway activation or in some cases if a negatively charged surface
25 induces contact activation (44). Protein surface adhesion may also form a passivating layer,
26 limiting any further inflammatory response. In the current study blood albumin and
27 fibrinogen concentrations were reduced on contact with the monoliths However, total
28
29
30
31
32
33
34
35
36
37
38
39
40
41
42
43
44
45
46
47
48
49
50
51
52
53
54
55
56
57
58
59
60

1
2
3 protein, albumin and fibrinogen concentrations all remained within the normal reference
4 range indicating a non-detrimental, dynamic, adsorptive equilibrium for these dominant
5 plasma proteins over the initial time course of haemodialysis. Adsorption of dominant
6 plasma protein serum albumin (66 kDa) and fibrinogen (340 kDa) did not prevent adsorption
7 of less concentrated high molecular weight IL-6 (28 kDa) and TNF- α (52 kDa), present in
8 picogram quantities, and adsorbed predominantly within the nanoporous domains of the
9 monoliths. The cause of this effect is not clear but could be related to the different
10 hydrophobic domains within the proteins. AC is a hydrophobic adsorbent and it has been
11 reported that the TNF- α trimer undergoes reversible dissociation into three monomeric
12 units in contact with hydrophobic surfaces and therefore smaller molecules of IL-6 and
13 TNF- α monomer (17 kDa) could be adsorbed predominantly within the nanoporous
14 domains of the monoliths inaccessible to albumin (45). Results confirm no significant impact
15 on total protein, electrolyte and haemolysis parameters using healthy donor blood perfused
16 through the small monoliths over time. Albumin and platelet reduction was slight using the
17 healthy blood samples in contrast to a previous study using post-haemodialysis blood
18 samples where a greater reduction in platelet count and albumin concentration was
19 observed (39). A number of additional variables including differences in blood sample
20 handling and monolith formulation may have influenced the heightened propensity for
21 haemodialysis blood sample proteins and platelets to adhere but the results also support
22 the premise that haemodialysis patient blood is primed for inflammation.

23
24
25
26
27
28
29
30
31
32
33
34
35
36
37
38
39
40
41
42
43
44
45
46
47
48
49
50 The haemocompatibility tests were carried out on the small monolith prototypes according
51 to ISO 10993 for blood contacting medical devices assessing platelet activation, granulocyte
52 activation, activation of t-cell intracellular phosphorylation pathways for STAT3 and STAT5
53 using flow cytometry, complement fragment concentration for C3a, C4a, C5a using ELISA
54
55
56
57
58
59
60

1
2
3 and coagulometry assays measuring pro-thrombin, APPT clotting times and fibrinogen
4
5 concentration. The signal transducer and activator of transcription (STAT) family are a group
6
7 of proteins activated by cytokines and growth factors through receptor associated kinase
8
9 phosphorylation followed by dimerization, translocation into the nucleus and transcription
10
11 of genes related to cell proliferation and the inflammatory response. They were used in this
12
13 study as the earliest indicator of T-cell activation on inflammatory stimulus by the
14
15 monoliths. Some complement activation and in particular granulocyte activation was
16
17 detected at the 60 minute time point for both monolith and tubing only negative controls.
18
19 Complement activation is known to occur routinely on exposure to a foreign surface within
20
21 haemodialysis, cardiopulmonary bypass and apheresis via the alternative pathway (46-48).
22
23 The small, cationic peptides C3a, C4a and C5a are anaphylatoxins which are free in the
24
25 plasma and bind to neutrophils and monocytes to promote ROS production, cytokine
26
27 release and cell hyper-adhesion. Activation was no more than the tubing only controls and
28
29 was markedly limited when compared to the zymozan A activated, positive control blood
30
31 samples, indicating that the artificial surfaces within the perfusion model itself and not the
32
33 monoliths promoted some activation of inflammatory pathways.
34
35

36
37 The large monoliths maintained adsorptive efficacy for the uraemic toxins IS and PCS and
38
39 cytokines IL-6 and TNF- α on scale up and at haemodialysis flow rates with minimal
40
41 pressure drop. Further work is required to establish breakthrough parameters and the
42
43 impact of rebound release on adsorption but the current study indicates that an adsorptive
44
45 equilibrium is maintained over 4 hours perfusion time. The broad spectrum adsorptive
46
47 capacity of the activated nanoporous carbon monoliths for organic molecules indicates that
48
49 these monoliths will have great capacity to remove other poorly removed protein bound
50
51 and middle molecule uraemic toxins from the growing family of uraemic toxins known to
52
53
54
55
56
57
58
59
60

1
2
3 remain after standard haemodialysis treatments and represented by these marker
4
5 molecules.
6

7
8 In summary, whilst haemodialysis patients have an immunosuppressive and altered
9
10 haemostatic balance so that blood cell fragility and inflammatory response on contact with
11
12 foreign surfaces will inevitably be hypersensitised toward inflammation (49) the results of
13
14 the current study show that, using healthy donor blood, a nanoporous activated carbon
15
16 monolith does not exacerbate blood cell activation according to ISO 10993
17
18 haemocompatibility measures. Haemocompatibility was also demonstrated using an in vivo
19
20 haemoperfusion safety model where no disruption of blood biochemistry or coagulopathy
21
22 occurred. The scaled up device maintained the internal nanoporous structure necessary to
23
24 augment haemodialysis efficacy through broad spectrum adsorption of small, protein bound
25
26 and high molecular weight uraemic toxins.
27
28
29

30 31 **5. Conclusion**

32
33 A novel lignin binder synthesis route has been used to synthesise nanoporous activated
34
35 carbon monoliths with maintained adsorptive capacity for marker protein bound and high
36
37 molecular weight toxins on scale up and testing at haemodialysis flow rates. These toxins
38
39 currently remain following haemodialysis and contribute to poor survival related to
40
41 cardiovascular disease and infection. The carbon monolith is safe and shows good
42
43 biocompatibility when tested in naive rats. Such a device could potentially be used as an in-line
44
45 haemoperfusion device to sit in line with and augment the clearance of uraemic toxins
46
47 poorly removed by standard haemodialysis.
48
49
50
51

52 53 54 55 **Acknowledgements**

56
57
58
59
60

1
2
3 All activated carbon monoliths were synthesised by MAST Carbon International, Jays Close,
4 Viables, Basingstoke, Hampshire, RG22 4BA, UK. This work is independent research funded
5 by the National Institute for Health Research, UK (Invention for Innovation (i4i), Product
6 Development Awards, II-LA-1111-20003). The views expressed in this publication are those
7 of the author(s) and not necessarily those of the NHS, the National Institute for Health
8 Research or the Department of Health. The work was supported by the NIHR Brighton &
9 Sussex Clinical Research Facility. The University of Brighton and UCL authors acknowledge
10 funding from the People Programme (Marie Curie Actions) of the European Union's Seventh
11 Framework Programme, Industry-Academia Partnerships and Pathways (IAPP) project
12 'Adsorbent Carbons for the Removal of Biologically Active Toxins' (ACROBAT-Grant
13 agreement no. 286366 FP7-People-2011-IAPP).
14
15
16
17
18
19
20
21
22
23
24
25
26
27
28
29
30

31 **References**

- 32
33
34 1. Saran R, Li Y, Robinson B, Ayanian J, Balkrishnan R, Bragg-Gresham J, et al. US Renal Data System
35 2014 Annual Data Report: Epidemiology of Kidney Disease in the United States. American journal of
36 kidney diseases : the official journal of the National Kidney Foundation. 2015;66(1 Suppl 1):Svii, S1-
37 305.
38
39 2. Ortiz A, Covic A, Fliser D, Fouque D, Goldsmith D, Kanbay M, et al. Epidemiology, contributors to,
40 and clinical trials of mortality risk in chronic kidney failure. Lancet. 2014;383(9931):1831-43.
41
42 3. Gansevoort RT, Correa-Rotter R, Hemmelgarn BR, Jafar TH, Heerspink HJ, Mann JF, et al. Chronic
43 kidney disease and cardiovascular risk: epidemiology, mechanisms, and prevention. Lancet.
44 2013;382(9889):339-52.
45
46 4. Vogelzang JL, van Stralen KJ, Noordzij M, Diez JA, Carrero JJ, Couchoud C, et al. Mortality from
47 infections and malignancies in patients treated with renal replacement therapy: data from the ERA-
48
49
50
51
52
53
54
55
56
57
58
59
60

1
2
3 EDTA registry. Nephrology, dialysis, transplantation : official publication of the European Dialysis and
4 Transplant Association - European Renal Association. 2015;30(6):1028-37.

5
6
7 5.El-Gamal D, Rao SP, Holzer M, Hallstrom S, Haybaeck J, Gauster M, et al. The urea decomposition
8 product cyanate promotes endothelial dysfunction. *Kidney international*. 2014;86(5):923-31.

9
10
11 6.Kwan JTC, Carr EC, Neal AD, Burdon J, Raftery MJ, Marsh FP, et al. Carbamylated hemoglobin, urea
12 kinetic modeling and adequacy of dialysis in hemodialysis-patients. *Nephrol Dial Transpl*.
13
14 1991;6(1):38-43.

15
16
17 7.Pietremont C, Gorisse L, Jaisson S, Gillery P. Chronic increase of urea leads to carbamylated
18 proteins accumulation in tissues in a mouse model of CKD. *Plos One*. 2013;8(12).

19
20
21 8.Velasquez MT, Ramezani A, Raj DS. Urea and protein carbamylation in ESRD: surrogate markers or
22 partners in crime? *Kidney international*. 2015;87(6):1092-4.

23
24
25 9.Eloot S, Van Biesen W, Glorieux G, Neiryck N, Dhondt A, Vanholder R. Does the adequacy
26 parameter Kt/V(urea) reflect uremic toxin concentrations in hemodialysis patients? *Plos One*.
27
28 2013;8(11):e76838.

29
30
31 10.Duranton F, Depner TA, Argiles A. The saga of two centuries of urea: Nontoxic toxin or vice versa?
32
33 *Semin Nephrol*. 2014;34(2):87-96.

34
35
36 11.Eloot S, Ledebro I, Ward RA. Extracorporeal removal of uremic toxins: can we still do better?
37
38 *Semin Nephrol*. 2014;34(2):209-27.

39
40
41 12.Vanholder R, Schepers E, Pletinck A, Nagler EV, Glorieux G. The uremic toxicity of indoxyl sulfate
42 and p-cresyl sulfate: a systematic review. *Journal of the American Society of Nephrology : JASN*.
43
44 2014;25(9):1897-907.

45
46
47 13.Shafi T, Meyer TW, Hostetter TH, Melamed ML, Parekh RS, Hwang S, et al. Free levels of selected
48 organic solutes and cardiovascular morbidity and mortality in hemodialysis patients: Results from
49 the retained organic solutes and clinical outcomes (ROSCO) investigators. *Plos One*.
50
51 2015;10(5):e0126048.
52
53
54
55
56
57
58
59
60

- 1
2
3 14. Wu IW, Hsu KH, Lee CC, Sun CY, Hsu HJ, Tsai CJ, et al. p-Cresyl sulphate and indoxyl sulphate
4 predict progression of chronic kidney disease. *Nephrology, dialysis, transplantation : official*
5 *publication of the European Dialysis and Transplant Association - European Renal Association.*
6
7 2011;26(3):938-47.
8
9
10
11 15. Sirich TL, Meyer TW, Gondouin B, Brunet P, Niwa T. Protein-bound molecules: a large family with
12 a bad character. *Semin Nephrol.* 2014;34(2):106-17.
13
14
15 16. Pletinck A, Glorieux G, Schepers E, Cohen G, Gondouin B, Van Landschoot M, et al. Protein-bound
16 uremic toxins stimulate crosstalk between leukocytes and vessel wall. *Journal of the American*
17 *Society of Nephrology.* 2013;24(12):1981-94.
18
19
20
21 22 17. Neiryck N, Vanholder R, Schepers E, Eloit S, Pletinck A, Glorieux G. An update on uremic toxins.
23 *Int Urol Nephrol.* 2013;45(1):139-50.
24
25
26 27 18. Duranton F, Cohen G, De Smet R, Rodriguez M, Jankowski J, Vanholder R, et al. Normal and
28 pathologic concentrations of uremic toxins. *Journal of the American Society of Nephrology : JASN.*
29 2012;23(7):1258-70.
30
31
32 33 19. Remuzzi G, Benigni A, Finkelstein FO, Grunfeld JP, Joly D, Katz I, et al. Kidney failure: aims for the
34 next 10 years and barriers to success. *Lancet.* 2013;382(9889):353-62.
35
36
37 38 20. Vanholder R, Boelaert J, Glorieux G, Eloit S. New methods and technologies for measuring
39 uremic toxins and quantifying dialysis adequacy. *Seminars in dialysis.* 2015;28(2):114-24.
40
41
42 43 21. Winchester JF. Haemoperfusion in the management of end-stage renal disease. *Life support*
44 *systems : the journal of the European Society for Artificial Organs.* 1984;2(2):107-11.
45
46 47 22. Winchester JF, Ronco C, Brady JA, Cowgill LD, Salsberg J, Yousha E, et al. The next step from high-
48 flux dialysis: application of sorbent technology. *Blood purification.* 2002;20(1):81-6.
49
50
51 52 23. Winchester JF, Silberzweig J, Ronco C, Kuntsevich V, Levine D, Parker T, et al. Sorbents in acute
53 renal failure and end-stage renal disease: middle molecule and cytokine removal. *Blood purification.*
54 2004;22(1):73-7.
55
56
57
58
59
60

- 1
2
3 24.Yatzidis H, Oreopoulos D. Early clinical trials with sorbents. *Kidney international Supplement*.
4
5 1976(7):S215-7.
6
7 25.Yatzidis H, Psimenos G, Mayopoulou-Symvoulidis D. Nondialyzable toxic factor in uraemic blood
8
9 effectively removed by the activated charcoal. *Experientia*. 1969;25(11):1144-5.
10
11 26.Yatzidis H, Yulis G, Digenis P. Hemocarboperfusion-hemodialysis treatment in terminal renal
12
13 failure. *Kidney international Supplement*. 1976(7):S312-4.
14
15 27.Andrade JD, Kopp K, Van Wagenen R, Chen C, Koliff WJ. Activated carbon and blood perfusion: a
16
17 critical review. *Proceedings of the European Dialysis and Transplant Association European Dialysis*
18
19 *and Transplant Association*. 1972;9(0):290-302.
20
21 28.Andrade JD, Kunitomo K, Van Wagenen R, Kastigir B, Gough D, Kolff WJ. Coated adsorbents for
22
23 direct blood perfusion: HEMA-activated carbon. *Transactions - American Society for Artificial Internal*
24
25 *Organs*. 1971;17:222-8.
26
27 29.Bartels O. Hemoperfusion through activated carbon adsorbent in liver-failure and hepatic-coma.
28
29 *Acta Hepato-Gastroenterologica*. 1978;25:324-9.
30
31 30.Botella J, Ghezzi PM, Sanz-Moreno C. Adsorption in hemodialysis. *Kidney international*
32
33 *Supplement*. 2000;76:S60-5.
34
35 31.Falkenhagen D, Gottschall S, Esther G, Courtney JM, Klinkmann H. In vitro assessment of charcoal
36
37 and resin hemoadsorbents. *Contributions to nephrology*. 1982;29:23-33.
38
39 32.Yang JB, Ling LC, Liu L, Kang FY, Huang ZH, Wu H. Preparation and properties of phenolic resin-
40
41 based activated carbon spheres with controlled pore size distribution. *Carbon*. 2002;40(6):911-6.
42
43 33.Gun'ko VM, Kozynchenko OP, Turov VV, Tennison SR, Zarko VI, Nychiporuk YM, et al. Structural
44
45 and adsorption studies of activated carbons derived from porous phenolic resins. *Colloid Surface A*.
46
47 2008;317(1-3):377-87.
48
49 34.Tennison SR. Phenolic-resin-derived activated carbons. *Appl Catal a-Gen*. 1998;173(2):289-311.
50
51 35.Howell CA, Sandeman SR, Phillips GJ, Lloyd AW, Davies JG, Mikhalovsky SV, et al. The in vitro
52
53 adsorption of cytokines by polymer-pyrolysed carbon. *Biomaterials*. 2006;27(30):5286-91.
54
55
56
57
58
59
60

- 1
2
3 36.Howell CA, Sandeman SR, Phillips GJ, Mikhalovsky SV, Tennison SR, Rawlinson AP, et al.
4
5 Nanoporous activated carbon beads and monolithic columns as effective hemoadsorbents for
6
7 inflammatory cytokines. *Int J Artif Organs*. 2013;36(9):624-32.
8
9
10 37.Sandeman SR, Howell CA, Mikhalovsky SV, Phillips GJ, Lloyd AW, Davies JG, et al. Inflammatory
11
12 cytokine removal by an activated carbon device in a flowing system. *Biomaterials*. 2008;29(11):1638-
13
14 44.
15
16 38.Sandeman SR, Howell CA, Phillips GJ, Lloyd AW, Davies JG, Mikhalovsky SV, et al. Assessing the in
17
18 vitro biocompatibility of a novel carbon device for the treatment of sepsis. *Biomaterials*.
19
20 2005;26(34):7124-31.
21
22 39.Sandeman SR, Howell CA, Phillips GJ, Zheng YS, Standen G, Pletzenauer R, et al. An adsorbent
23
24 monolith device to augment the removal of uraemic toxins during haemodialysis. *J Mater Sci-Mater*
25
26 *M*. 2014;25(6):1589-97.
27
28
29 40.Pavlenko D, van Geffen E, van Steenberg MJ, Glorieux G, Vanholder R, Gerritsen KG, et al. New
30
31 low-flux mixed matrix membranes that offer superior removal of protein-bound toxins from human
32
33 plasma. *Sci Rep*. 2016;6.
34
35 41.Tripisciano C, Kozynchenko OP, Linsberger I, Phillips GJ, Howell CA, Sandeman SR, et al.
36
37 Activation-Dependent Adsorption of Cytokines and Toxins Related to Liver Failure to Carbon Beads.
38
39 *Biomacromolecules*. 2011;12(10):3733-40.
40
41
42 42.Presser V, Yeon SH, Vakifahmetoglu C, Howell CA, Sandeman SR, Colombo P, et al. Hierarchical
43
44 Porous Carbide-Derived Carbons for the Removal of Cytokines from Blood Plasma. *Adv Healthc*
45
46 *Mater*. 2012;1(6):796-800.
47
48
49 43.Gilbert RJ, Park H, Rasponi M, Redaelli A, Gellman B, Dasse KA, et al. Computational and
50
51 functional evaluation of a microfluidic blood flow device. *ASAIO journal*. 2007;53(4):447-55.
52
53 44.van Oeveren W. Obstacles in haemocompatibility testing. *Scientifica*. 2013;2013:392584.
54
55 45.Kunitani MG, Cunico RL, Staats SJ. Reversible subunit dissociation of tumor necrosis factor during
56
57 hydrophobic interaction chromatography. *Journal of chromatography*. 1988;443:205-20.
58
59
60

1
2
3 46.Kourtzelis I, Markiewski MM, Doumas M, Rafail S, Kambas K, Mitroulis I, et al. Complement
4 anaphylatoxin C5a contributes to hemodialysis-associated thrombosis. *Blood*. 2010;116(4):631-9.
5
6

7 47.Kourtzelis I, Rafail S, DeAngelis RA, Foukas PG, Ricklin D, Lambris JD. Inhibition of biomaterial-
8 induced complement activation attenuates the inflammatory host response to implantation. *FASEB*
9 *journal : official publication of the Federation of American Societies for Experimental Biology*.
10 2013;27(7):2768-76.
11
12
13
14

15 48.Rousseau Y, Haeffner-Cavaillon N, Poinet JL, Meyrier A, Carreno MP. In vivo intracellular
16 cytokine production by leukocytes during haemodialysis. *Cytokine*. 2000;12(5):506-17.
17
18

19 49.Friedrich B, Alexander D, Janessa A, Haring HU, Lang F, Risler T. Acute effects of hemodialysis on
20 cytokine transcription profiles: evidence for C-reactive protein-dependency of mediator induction.
21 *Kidney international*. 2006;70(12):2124-30.
22
23
24
25
26
27
28
29
30
31
32
33
34
35
36
37
38
39
40
41
42
43
44
45
46
47
48
49
50
51
52
53
54
55
56
57
58
59
60